Published in final edited form as:
Neuroscience. 2014 March 7; 261: 74–84. doi:10.1016/j.neuroscience.2013.12.033.

Melatonin in the mammalian olfactory bulb

J.T. Corthell[1,*], **J. Olcese**[2], and **P.Q. Trombley**[1]

[1]Florida State University, Department of Biological Science, Program in Neuroscience, Tallahassee, FL 32306.

[2]Florida State University, Department of Biomedical Sciences, Program in Neuroscience, Tallahassee, FL 32306.

Abstract

Melatonin is a neurohormone associated with circadian rhythms. A diurnal rhythm in olfactory sensitivity has been previously reported and melatonin receptor mRNAs have been observed in the olfactory bulb, but the effects of melatonin in the olfactory bulb have not been explored. First, we corroborated data from a previous study that identified melatonin receptor messenger RNAs in the olfactory bulb. We then investigated whether melatonin treatment would affect cells in the olfactory bulbs of rats. Using a combination of PCR, qPCR, cell culture, and electrophysiology, we discovered that melatonin receptors and melatonin synthesis enzymes were present in the olfactory bulb and we observed changes in connexin43 protein, GluR1 mRNA, GluR2 mRNA, Per1 mRNA, Cry2 mRNA, and K^+ currents in response to 2-iodomelatonin. Via qPCR, we observed that messenger RNAs encoding melatonin receptors and melatonin biosynthesis enzymes fluctuated in the olfactory bulb across 24 hours. Together, these data show that melatonin receptors are present in the olfactory bulb and likely affect olfactory function. Additionally, these data suggest that melatonin may be locally synthesized in the olfactory bulb.

Introduction

Melatonin is a lipophilic neurohormone that signals the onset of darkness. Melatonin affects circadian rhythms in animals that generate melatonin (Hunt et al., 2001; reviewed in Pandi-Perumal et al., 2006, and Zawilska et al., 2009). A previous study (Granados-Fuentes et al., 2011) reported a diurnal rhythm in olfactory discrimination behavior that was sensitive to the knockout of some clock genes. Melatonin can affect different clock genes, and melatonin receptor mRNAs have been previously reported in the olfactory bulb (OB; Ishii et al., 2009). We wanted to determine if melatonin administration could affect the olfactory system. However, melatonin can act via direct binding to intracellular proteins (Nosjean et al., 2000) or membrane-bound G-protein-coupled receptors. Much more is known about the effects of melatonin binding to its receptors, and we chose to focus our investigations there.

[*]Corresponding author. 238 Biomedical Research Facility, Florida State University, Tallahassee, FL 32306-4340. corthell@neuro.fsu.edu, 850-644-1616.

Author contributions: J.T. Corthell, J. Olcese, and P.Q. Trombley designed experiments; J.T. Corthell and P.Q. Trombley performed experiments; J.T. Corthell analyzed the data and performed statistical analysis; J.T. Corthell, J. Olcese, and P.Q. Trombley wrote the manuscript.

Membrane-bound melatonin receptors, in mammals, come in two isoforms: melatonin receptor 1 (MT1R; also called MTNR1a) and melatonin receptor 2 (MT2R; also called MTNR1b). A third putative isoform, melatonin receptor 3, was revealed to be the intracellular protein quinone reductase 2 (Nosjean et al., 2000). Melatonin receptors (reviewed by Dubocovich et al., 2010) are 7-transmembrane domain proteins, attached to G-proteins (G_i/G_o) that interact with adenylyl cyclase, leading to a dephosphorylation of cAMP response element-binding protein and/or changes in mitogen-activated protein kinase or mitogen-activated protein kinase kinase, and therefore changes in transcription and translation of different genes, including entrainment of the SCN clock (Lee et al., 2010). Melatonin receptors can also indirectly interact with K^+ channels in the suprachiasmatic nucleus of the hypothalamus (SCN; Inyushkin et al., 2007) and K^+ channels and glycine receptors in the retina (Yang et al., 2011; Zhao et al., 2010). Melatonin receptors are involved in the circadian timing of some behaviors in different species, mostly via receptors expressed by SCN cells. Messenger RNAs encoding MT1R and MT2R were previously reported in the OB of rats (Ishii et al., 2009), but these data, to date, have not been corroborated or further explored. The OB is similar to the retina by virtue of its laminar organization and function in initial sensory processing, while the OB is similar to the SCN and the retina because the OB has circadian rhythms in gene expression and electrical activity that continue without outside input (Granados-Fuentes et al., 2004); due to these similarities, we chose to focus our investigation on known actions of melatonin in the SCN and the retina and to examine if melatonin's actions in the OB were similar.

Odorant processing begins in the mammalian OB after odorants bind to receptors in the olfactory mucosa of the nose. A message from the nose is sent by olfactory sensory neuron axons, which form the olfactory nerve layer (ONL) of the OB, and project to structures called glomeruli in the glomerular layer (GL) of the OB. Juxtaglomerular (JG) cells surround glomeruli and can be subdivided into periglomerular (PG), short-axon (SA), and external tufted (ET) cells, along with some histologically unidentified cell types (Kosaka and Kosaka, 2011). The principal output neurons of the OB are mitral cells in the mitral cell layer (MCL) and tufted cells in the external plexiform layer of the OB. Finally, granule and Blanes cells reside in the granule cell layer (GCL). A subset of the PG cells and the majority of cells in the GCL release the inhibitory neurotransmitter gamma-amino butyric acid (GABA) and inhibit mitral and tufted cell activity.

Melatonin itself is released from the pineal gland into the bloodstream (though the retina and other tissues have been reported to synthesize melatonin; see Gomez-Corvera et al., 2009, and Itoh et al., 2007), and is synthesized from serotonin by two enzymes: arylalkylamine N-acetyltransferase (AANAT) and hydroxyindole-O-methyltransferase (HIOMT; also called acetylserotonin methyltransferase, or ASMT). AANAT mRNA has been shown in the OB (Uz et al., 2002). HIOMT mRNA has been shown in multiple brain areas, but not in the OB (Ribelayga et al., 1998).

We pursued three hypotheses for this study, using a combination of PCR, qPCR, immunoblotting, cell culture, immunohistochemistry, and electrophysiology: first, that melatonin receptors and HIOMT are present in the OB; second, that melatonin receptors and melatonin biosynthesis enzymes fluctuate over 24 hours; and third, that melatonin receptor activation mediates transcriptional, translational, and electrical changes in OB cells.

1. Experimental Procedures

1.1. Animals

Male and female Sprague Dawley rat pups, aged postnatal days 21–23, (Charles River, Raleigh, NC) were kept in standard rat cages under a 12-hr light, 12-hr dark cycle (lights on

at 0700 h EST; ZT0). Water and rat chow were available *ad libitum*. Male and female wild-type, melatonin receptor 1 knock-out (MT1RKO; Liu et al., 1997), melatonin receptor 2 knock-out (MT2R-KO; Jin et al., 2003), and MT1RKO/ MT2R-KO mice (C3H strain) were provided by the Olcese laboratory at Florida State University. MT1R-KO and MT2R-KO mice were genotyped and assayed for MT1R and MT2R transcripts by sequencing using a HiSeq sequencer (Illumina, San Diego, CA) to ensure that KO animals did not express melatonin receptors. For tissue collection, animals were anesthetized using isoflurane and killed by decapitation. During the night, tissue collection was performed under dim red light. For immunohistochemical samples, animals were anesthetized with a mixture of ketamine and xylazine and killed by transcardial perfusion. The animals for these experiments were used according to the guidelines of our protocol approved by Florida State University's Animal Care and Use Committee and the National Institutes of Health Guide for the Care and Use of Laboratory Animals (NIH Publications No. 80–23).

1.2. RNA Extraction

Rat pups of ages P21, P22, and P23 were killed at 3-h intervals over 48-h and their OBs were excised and placed immediately in RNAlater reagent (Qiagen, Valencia, CA) according to manufacturer's instructions. For processing, samples were removed from RNAlater, placed in ice-cold TRIzol reagent (Life Technologies, Carlsbad, CA), and homogenized with a rotor-stator homogenizer (PRO Scientific, Oxford, CT) at 50% amplitude with autoclaved probes washed in diethylpyrocarbonate-treated water. Samples homogenized in TRIzol were processed according to manufacturer's instructions with the following changes: the chloroform-addition step was repeated, samples in isopropanol were left at −20°C overnight, and the samples were not heated for resuspension. The resulting pellet was resuspended in 100 µl of RNase-, DNase-free water (EMD Millipore, Billerica, MA) and processed through the RNEasy Mini Kit (Qiagen) according to the manufacturer's RNA Cleanup protocol with DNase I treatment (Qiagen). Purified RNA samples were spun for 40 min in a vacuum concentrator and stored at −20°C until use.

1.3. Reverse transcription, PCR, and quantitative PCR

Purified RNA samples were kept on ice and their concentrations assayed with a Nanodrop 1000 spectrophotometer (Thermo Scientific, Rockford, IL). Sample integrity was assayed by gel electrophoresis with SYBR Safe DNA Dye (Life Technologies). Five µg of total RNA from tissue or 2 µg of total RNA from MOB brain slices were used for the reverse-transcription reaction with a Superscript III Reverse Transcription Supermix Kit (Life Technologies), according to the manufacturer's instructions except for inclusion of both random oligonucleotides and $oligo_{dT(20)}$ as primers for the reverse transcription, from the protocol of Resuehr and Speiss (2003). The resulting cDNA was diluted 1:10 in RNase-, DNase-free water.

Polymerase chain reaction (PCR) solutions were composed of HotStarTaq Master Mix (Qiagen), 2 µl of the diluted cDNA, and 500 nM primers, according to manufacturer instructions. PCR was run on a Veriti thermal cycler (Life Technologies). Reactions were run as follows: 95°C for 15 min; 40 cycles of 94°C for 30 s, 55°C for 1 min, and 72°C for 1 min; 72°C for 10 min, 4°C until samples were prepared for gel electrophoresis. PCR products were analyzed using 1.6% agarose gel electrophoresis in Tris-boric acid-EDTA buffer (TBE) and run at 43V for 90 minutes, visualized using a Gel Doc XR+ system (Bio-Rad, Hercules, CA). PCRs in which diluted cDNA was replaced with water did not show bands on electrophoresis gels. PCRs in which diluted cDNA was replaced with RNA (no reverse transcription) did not show bands on electrophoresis gels.

The quantitative PCR solution was composed of Power SYBR Green Master Mix (Life Technologies), 2 μl of the diluted cDNA, and 500 nM primers, according to manufacturer instructions. The quantitative PCR reactions were run on a 7500Fast Real-Time PCR Thermocycler (Life Technologies). All reactions were run as follows: 50°C for 2 min, 95°C for 10 min; 40 cycles of 95°C for 15 s and 60°C for 1 min; melt curve analysis. Ribosomal protein S28, β-III-tubulin, and glyceraldehyde-3-phosphate dehydrogenase (GAPDH) mRNAs were used as reference genes. Each reaction plate also contained a sample of pooled cDNA as a reference value to allow comparisons between multiple plates. Reactions were compared to each of the reference genes, and line plots for each reference were similar. Reference genes were compared to each other and both β-III-tubulin and GAPDH mRNAs did not show significant fluctuation. Control reactions where cDNA was replaced with water did not reach the critical threshold. Control reactions where cDNA was replaced with RNA (no reverse transcription) did not reach critical threshold. Reported results use GAPDH as the reference gene.

1.4 Primer Design and Primers Used

Primer sets for *MT1R*, *MT2R*, *aromatic L-amino acid decarboxylase* (AADC, also called DOPA decarboxylase), *tryptophan hydroxylase isoform 2* (TPH2), and *AANAT*, shown in Table 1, were designed with OligoExplorer freeware (http://www.genelink.com/tools/gl-oe.asp), reanalyzed with NetPrimer software (Premier Biosoft, Palo Alto, CA), and ordered from Integrated DNA Technologies (Coralville, IA). Only primer sets that did not form dimers or hairpins *in silico* were used. The products were then submitted as a BLAST (NCBI, http://blast.ncbi.nlm.nih.gov/Blast.cgi) query against RefSeqmRNA in the *Rattus norvegicus* genome. Any primer sets with nonspecific products were not used. The GAPDH primer set was designed to span between exons 3 and 4 and therefore serve as a check for DNA contamination through the appearance of introns, and this was confirmed by PCR. We tested quantitative PCR products by melt curve, sequencing, and agarose gel electrophoresis to ensure specificity and correct band size. The primer sets for AMPAR subunits *GluR1–4* were as published by Santiago et al. (2009), primer sets for *Cx36*, *Cx43*, and *Cx45* were as published byCorthell et al. (2012), the primer set for *tryptophan hydroxylase isoform 1* (TPH1) were published by Sugden (2003), the primer set for *HIOMT* was as published by Sanchez-Hidalgo et al. (2009), and the primer sets for the clock genes *Clock*, *Bmal1*, *Period1* (Per1), *Period2* (Per2), *Period3* (Per3), *Cryptochrome1* (Cry1), *Cryptochrome2* (Cry2), *Rev-erb* α, *Rev-erb* β, and *ROR*α were as published byKamphuis et al. (2005). Sequencing of PCR and qPCR products was performed by the Florida State University Biology Core facility staff.

1.5 Membrane Preparation

Rat pups (P21) were killed at 3-h intervals over a 24-h period, and their OBs and hippocampi were dissected and placed immediately in a dry-ice/95%-ethanol slurry for flash-freezing. OBs from the wild-type, MT1R-KO, and MT2R-KO mice were harvested similarly but without regard to time. All samples were stored at −80°C until processing. Before processing, protease inhibitors were added to a homogenization buffer (320 mM sucrose, 1 mM EDTA, 50 mM KCl, 10 mM Tris base, 1 μg/ml leupeptin, 1 μg/ml pepstatin A, 2 μg/ml aprotinin, 1 mg/ml phenylmethylsulfonyl fluoride, pH 7.8; all from Sigma-Aldrich, St. Louis, MO), and then samples were homogenized by 50 strokes on ice with a Kontes 20 tissue grinder. Each sample was a pair of OBs or hippocampi from a single rat or mouse. Membrane proteins were purified by two rounds of low-speed centrifugation (6,500 g for 10 minutes at 4°C) and then one high-speed centrifugation (107,000 g for 30 minutes at 4°C) with an Optima MAX-XP (Beckman-Coulter, Brea, CA) in a protocol adapted fromGuillemin et al. (2005) and Schindler et al. (2006). The pellet was reconstituted by tip

sonication (Model 120, Fisher Scientific, Pittsburgh, PA) as previously described (Cook and Fadool, 2002) and stored at −80°C until use.

1.6 Sodium Dodecyl Sulfate-Polyacrylamide Gel Electrophoresis (SDS-PAGE) and Immunoblotting

Protein concentrations were determined using a Bradford assay (Bio-Rad). Proteins were separated by 10% polyacrylamide gel electrophoresis with 30 μg total membrane protein per sample then electrotransferred to polyvinylidene fluoride membranes (Millipore) by wet transfer using ice-cold solutions described by Sambrook and Russell (2001) and treated with anti-melatonin receptor antisera. Blots were visualized by autoradiography with ECL Plus reagents (GE Healthcare, Piscataway, NJ). Blots were stripped with the stripping buffer described by Yeung and Stanley (2009) and reprobed with rabbit monoclonal anti-β-III-tubulin (Cell Signaling Technology, Beverly, MA) as a loading control. Antisera used as markers in immunohistochemistry (IHC) were tested by immunoblot (10 μg total membrane protein per sample) as an additional control; calretinin, parvalbumin, GAD65, and GAD67 blots showed single bands at the appropriate weights, while the tyrosine hydroxylase blot showed 3 bands that were all explained by the data sheet and therefore expected. For samples to be processed by mass spectrometry, polyacrylamide gels were stained using Coomassie Blue and the resulting bands of appropriate weights were cut out and submitted to the Florida State University College of Medicine Translational Laboratory for mass spectrometry analysis.

1.7 Transcardial Perfusion, Fixation, and Slicing

Rats were anesthetized by a mixture of ketamine and xylazine and transcardially perfused first by 0.9% saline/0.1% heparin, followed by 4% paraformaldehyde/2.5% acrolein, while mice were anesthetized by a mixture of ketamine and xylazine and transcardially perfused first by 0.9% saline, followed by 4% paraformaldehyde. Whole brains were removed and placed into 10 ml of the same fixative used for perfusion for 4 hours. Brains were then placed into autoclaved 30% sucrose solution until the brains sank, after which they were removed from the sucrose solution and sliced into 50 μm-thick horizontal sections of OB or coronal sections of hippocampus on a freezing-stage microtome (Thermo Fisher) with a temperature controller (Physitemp, Clifton, NJ) and placed into a cryoprotectant solution (Hoffman et al., 2008) at −20°C until they were examined by immunohistochemistry.

1.8 Immunohistochemistry (IHC)

Slices were removed from cryoprotectant and processed as described byHoffman et al. (2008). Briefly, slices were washed in 0.1M phosphate buffered saline (PBS), incubated in 1% sodium borohydride solution, washed in PBS, and blocked in 1% horse, goat, or donkey serum, depending on the secondary antibody being used, and incubated in primary antibody for 48 hours at 4°C. For reactions to be visualized using nickel-diaminobenzidine (Ni-DAB) chemistry, samples were washed in PBS after primary antibody incubation and treated for 2 hours with a biotinylated secondary antibody and processed using an avidin-biotin complex kit (Vector Laboratories) and Ni-DAB. For reactions to be visualized using fluorescence with a confocal microscope, samples were washed in PBS after primary antibody incubation and treated for 2 hours with biotinylated and fluorescent secondary antibodies, washed in PBS, and treated for 1 hour with fluorophore-conjugated streptavidin. Slices were treated with Gel-Mount (Sigma-Aldrich) to preserve fluorescence. Ni-DAB slices were examined under light microscopy and fluorescence slices were examined using a SP2 confocal microscope (Leica, Wetzlar, Germany). Electrophysiology slices with biocytin-filled cells were immersion-fixed in 4% paraformaldehyde, washed in 0.1M PBS, treated with Cy3-conjugated streptavidin, and examined using a fluorescent microscope (Leica).

1.9 Antisera

For IHC, antibodies were titrated as described byHoffman et al. (2008). For immunoblotting, antibodies were titrated by dilution series, starting at the manufacturer's instructions, and diluted in 1–4% nonfat dry milk diluted in 0.1% Tween-20/Tris-buffered saline (TBST). For IHC, antibodies were diluted in 1% serum diluted in PBS/0.4% Triton X-100. Primary antisera used in this study were the following: rabbit anti-MT1R (1:1000 in 1% milk/TBST; Abbiotec, 250761), rabbit anti-MT1R (1:1000 in 4% milk/TBST; 1:3000 in Ni-DAB IHC; Novus, NBP1-71113), goat anti-MT2R (1:500 in 4% milk/TBST; Santa Cruz, sc-13177), rabbit anti-MT2R (1:1000 in 4% milk/TBST, 1:10,000 in Ni-DAB IHC, 1:500 in fluorescent IHC (FIHC) using streptavidin and a biotinylated secondary antibody; Novus, NLS932), mouse antityrosine hydroxylase (1:30,000 in FIHC; Chemicon, MAB318), mouse anti-glutamic acid decarboxylase (GAD)-65 (1:10,000 in FIHC; Abcam, ab26113), mouse anti-GAD67 (1:10,000 in FIHC; Chemicon, MAB5406), goat anti-calretinin (1:30,000 in FIHC; Chemicon, AB1550), goat anti-parvalbumin (1:2000 in FIHC; Swant, PVG-214), rabbit monoclonal anti-β-III-tubulin (1:2000 in 4% milk/TBST; Cell Signaling Technology, 5568), and rabbit anti-connexin43 (1:1000 in immunocytochemistry; Millipore AB1728). Secondary antibodies used in this study were the following: horseradish peroxidase (HRP)-conjugated goat anti-rabbit (1:10,000 in 4% milk/TBST; Bio-Rad 170-5046), HRP-conjugated goat antimouse (1:10,000 in 4% milk/TBST; Bio-Rad 170-5047), HRP-conjugated donkey anti-goat (1:40,000 in 1% milk/TBST; Jackson ImmunoResearch, 705-035-001), biotinylated horse anti-rabbit (1:1000, Vector, BA-1100), biotinylated horse anti-goat (1:1000, Vector, BA-9500), biotinylated goat anti-rabbit (1:1000, Jackson ImmunoResearch), biotinylated goat anti-mouse (1:1000, Jackson ImmunoResearch, 115-065-003), fluorescein-conjugated horse anti-mouse (1:1000, Vector, FI-2000), Cy3-conjugated goat anti-rabbit (1:1000, Jackson ImmunoResearch, 111-165-144), and Cy3-conjugated donkey anti-goat (1:1000, Jackson ImmunoResearch, 705-165-147). Both Cy3-(Jackson ImmunoResearch, 016-160-084) and Alexa488-conjugated (Life Technologies, S32354) streptavidin were used at 1:1000 in this study, diluted in 0.4% Triton X-100/PBS for FIHC.

1.10 Tissue Culture

Rat pups aged P1-P3 were sacrificed and their OBs dissected and dissociated, as previously described (Trombley and Blakemore, 1999). Cells were grown in a 75 ml flask and knocked after 3 days in culture. Knocking the flask removes most non-astrocytic OB cells and therefore 'enriches' for astrocytes. After knocking, cells were grown until confluence, after which they were split into multiple dishes and grown to near confluence on coverslips. After reaching about 80% confluence, a mitotic inhibitor (FUDR; Sigma-Aldrich) was added to the culture medium. One day after addition of the mitotic inhibitor, cultures were treated with 3 nM 2-iodomelatonin (I-mel; Tocris Bioscience, Bristol, UK) for 4 hours. I-mel was chosen because I-mel is more stable than melatonin, I-mel has a higher affinity for melatonin receptors than melatonin, and the iodide moiety should prevent melatonin from passing through cell membranes, and therefore any effects of I-mel should be mediated by the membrane-bound receptors. After treatment, cells were fixed, treated with rabbit anti-Cx43 and processed for fluorescent immunocytochemistry in a similar manner to FIHC. Fluorescence was analyzed using ImageJ software (NIH).

1.11 Brain slice collection

OB slices were prepared from 10- to 28-day-old Sprague-Dawley rats that had been anesthetized with isoflurane and then killed by decapitation. OBs were rapidly removed and placed in ice-cold oxygenated (95% O_2-5% CO_2) high-sucrose saline solution. Horizontal slices (400 μm) were made using a vibratory microtome (Vibratome, St. Louis, MO) and incubated in a holding chamber for 30 min at 35°C. Slices were then stored at 20–24°C until

use. For electrophysiology, slices were placed into a recording chamber and viewed using a Leica microscope (Leica) equipped with infrared differential interference contrast optics. Mitral and JG cells were discriminated on the basis of morphology and location within the slice. Slices were either used for electrophysiological study or treated with either 4 nM I-mel (diluted in DMSO) or control solution that contained an equivalent amount of DMSO (0.01%). Slices in the I-mel experiment were treated for 4 hours and placed into RNAlater until RNA extraction.

1.12 Electrophysiology

Whole cell patch-clamp recordings were obtained from JG and mitral cells in OB slices using methods similar to those we and others have described previously (Blakemore et al., 2006). Recordings were obtained using an Axoclamp 700B amplifier (Molecular Devices, Sunnyvale, CA) and Axograph software (Axograph, Berkeley, CA) in continuous voltage-clamp mode. The extracellular solution was oxygenated (95% O_2-5% CO_2) and contained (in mM) 125 NaCl, 25 $NaHCO_3$, 1.25 NaH_2PO_4, 25 glucose, 2.5 KCl, 1.0 $MgCl_2$, and 2 $CaCl_2$, pH 7.3. Patch pipettes were pulled to a resistance of 1–3 MΩ. Inhibitory postsynaptic current (IPSC) measurements were performed using a pipette solution containing (in mM) 125 $KMeSO_4$, 2 $MgCl_2$, 0.025 $CaCl_2$, 1 EGTA, 2 Na^+-ATP, 0.5 Na^+-GTP, 5 Na^+-phosphocreatine, 0.2% biocytin hydrochloride, and 10 HEPES, pH 7.3, osmolarity adjusted to 280 mOsm using $KMeSO_4$. Recordings were obtained in the presence of 1 μM tetrodotoxin (TTX) to block Na^+ currents, or 1 μM TTX and 100 nM I-mel to record the effects of melatonin receptor activation. Drugs were applied by bath perfusion. To evaluate K^+ currents, we examined cell responses to a series of voltage steps, +10 mV each for 150 ms, from a holding current of −60 mV (−50 mV to +20 mV). To evaluate the contribution of A13 type K^+ currents, we examined cell responses to a combined hyperpolarization/depolarization protocol, where cells were held at −60 mV, hyperpolarized to −80 mV for 25 ms, and depolarized from −80 to +20 mV for 150 ms. We also examined cell responses to a −10 mV hyperpolarization for 100 ms to record changes in membrane resistance.

1.13 Statistical Analysis

Circadian data collected by qPCR were evaluated by Kruskal-Wallis nonparametric ANOVA, Dunn's post-hoc, and Pearson's product-moment correlation tests. I-mel treatment data were evaluated by Student's t-test, compared to controls. Electrophysiology data were evaluated by Student's t-test, compared to controls. For all tests, significance was declared for any test with a resulting p-value less than 0.05.

2 Results

2.1 Messenger RNAs encoding melatonin receptors and synthesis enzymes are present in the OB

While Ishii et al. (2009) reported melatonin receptor mRNAs in the rat OB, those data had not been corroborated. Additionally, AANAT had been observed in the OB (Uz et al., 2002), but HIOMT had not. We began our studies by asking if melatonin receptors and HIOMT were present in the OB. The results of our PCR and agarose gel electrophoresis (Figure 1A) show that mRNAs encoding MT1R, MT2R, and the entire melatonin biosynthesis pathway are present in rat OB tissue. We then examined if proteins for the melatonin receptors were present, by immunoblotting and IHC. We tested two antibodies against MT1R and two against MT2R (data not shown). For each antibody, all immunoreactive bands disappeared when the primary antibody was omitted or incubated in the presence of an excess of the antigen protein; however, all immunoreactive bands that were present in the wild-type OB and hippocampus samples were also present in the samples from the knock-out mice. Bands corresponding to the weights of the immunoreactive bands were submitted for mass

spectrometry, which found that none of the four bands tested (38, 50, 76, and 150 kDa) had MT1R, MT2R, or melatonin-related receptor proteins; the 76 kDa band had HIOMT protein in 2 of the 3 samples, 95% confidence.

We tested those same antibodies in IHC and found that only the rabbit anti-MT2R (Novus) gave good results (Figure 1B). Staining disappeared in rat and mouse OB tissue when the primary antibody was omitted, as well as in a 20x excess of antigen protein; however, staining was similar between wild-type and MT2R-KO tissue. Interestingly, the antibody appears to be a unique histological marker for OB JG cells, as anti-MT2R did not produce significant co-labeling in FIHC with antibodies to tyrosine hydroxylase, calretinin, GAD65, GAD67, or parvalbumin proteins (data not shown), and was not similar to calbindin or neurocalcin labeling previously reported (Briñón et al., 1998; Hwang et al., 2002).

2.2 Melatonin receptor mRNAs and synthesis enzyme mRNAs fluctuate over time in the OB

We tested if MT1R and MT2R expression fluctuated in the OB as they do in the SCN. The results are shown in Figure 2. MT1R mRNA fluctuates over 48 hours but does not appear to be rhythmic. MT2R mRNA does show large changes but the changes did not occur at the same time between the two 24-hour periods. The enzymes were examined over 24-hour periods and show fluctuations, shown in Figure 3. AANAT primers, while specific for PCR, failed some controls in qPCR and the data were thus discarded. When compared to each other, β-III-tubulin and GAPDH mRNAs did not fluctuate (data not shown). Kruskal-Wallis and Dunn's analyses showed that TPH2, AADC, and HIOMT mRNAs had statistically significant differences between groups ($p < 0.05$); these same mRNAs had statistically significant differences between the light and dark phases. Additionally, correlation analysis of the 5 synthesis genes suggests correlations between TPH1 and AADC ($c = 0.480$), TPH1 and HIOMT ($c = 0.569$), and AADC and HIOMT ($c = 0.897$). All 3 had $p < 0.05$ in Pearson's test.

2.3 Activation of melatonin receptors results in transcriptional and translational changes

We wanted to examine if OBs would respond to I-mel to determine if melatonin receptors were present in the OB and simply could not be detected by our previous methods. Previous reports have indicated that melatonin can affect the expression of connexin proteins and clock genes (Sharkey et al., 2009; Zeman and Herichova, 2013), and may affect the expression of glutamate receptor subunits (Corthell et al., 2012). Figure 4 shows that OB primary cell cultures, when treated with I-mel, increase in connexin43 protein expression and show a more diffuse pattern of expression than controls. Analysis of OB slices by qPCR (Figure 5) showed that I-mel reliably decreased GluR1, GluR2, Per1, and Cry2 mRNAs (t-test, $p < 0.05$) but did not appear to affect Bmal1 mRNA expression. Connexin36, connexin 43, connexin45, GluR3, GluR4, Per2, Per3, Cry1, RORα, Rev-erb α, Rev-erb β, MT1R, and MT2R mRNAs were also tested but changes were inconsistent (data not shown). These data demonstrate that melatonin receptors are present in the OB and mediate transcriptional and translational changes in OB cells.

2.4 Iodomelatonin alters K^+ currents in a subset of juxtaglomerular cells

We decided to test two major cell populations of the OB for responses to I-mel: mitral and JG cells. We first tested mitral cells in the OB for responses to 100 nM I-mel ($n = 4$). Mitral cells did not appear to respond to melatonin in any meaningful way. We then patched JG cells in the GL ($n = 12$) and found that a subset of JG cells show decreases in K^+ current in response to I-mel that washes out in 5–10 minutes (Figure 6; $n = 3$ for washout). In these JG cells, I-mel application reduced K^+ currents to 82 +/− 6% of control within 5 minutes, and to 77 +/− 4% of control within 10 minutes, recovering to 90+/− 6% within 5 minutes of washout (averages +/− SEM). I-mel application did not induce any currents by itself during

5 minutes of recording in any of the cells we examined (data not shown). We also examined cell responses to a hyperpolarizing pulse followed by depolarization; the pattern of those data was identical to the changes observed in the voltage step protocol (data not shown).

3 Discussion

Our data suggest that melatonin receptors are present in the mammalian OB and that they affect OB function. Activation of these receptors appears to affect 3 mRNAs and a protein that have been previously identified as fluctuating over time (Per1, GluR1, GluR2, and connexin43; Corthell et al., 2012; Granados-Fuentes et al., 2004). Changes in the AMPA receptor subunits GluR1 and GluR2 are interesting because of the effects that AMPA receptors have in the SCN and the MOB, especially Ca^{2+}- permeable AMPA receptors (Blakemore et al., 2006; Ma and Lowe, 2007; Michel et al., 2002; Paul et al., 2005; Pimentel and Margrie, 2008; Schoppa and Westbrook, 2002). Additionally, I-mel application affects K^+ currents in an unidentified subset of JG cells. It is not clear if these JG cells are the only cells that express melatonin receptors, or if they are the only cells that express melatonin receptors that indirectly interact with K^+ channels in the OB; we did not examine granule cells to determine if they expressed melatonin receptors. Because we used whole OB preparations for our transcriptional and translational experiments, the cells responsible for the effects of melatonin that we observed remain to be determined. Serotonin and melatonin do not bind to each other's receptors, and thus we do not consider our observations to be due to activation of serotonin receptors (Dubocovich et al., 2010; Krause and Dubocovich, 1991). Finally, melatonin receptors may have been in the bands submitted for mass spectrometry, but at concentrations below detection threshold; we do not think that this changes our conclusions regarding the antibodies used to detect melatonin receptors.

The presence of HIOMT mRNA and protein suggests that melatonin may, in addition to the brain's pineal gland and retina, be synthesized in the OB. We hypothesize that OB melatonin synthesis occurs after the OB receives serotonergic stimulation from the dorsal raphe nuclei. Past research has shown that histological staining for serotonin does not stain OB cells but stains dorsal raphe afferents (McLean and Shipley, 1987). Because of this, we believe that the TPH1 and TPH2 mRNAs we observed were in those afferents and not OB cells. AADC is involved in dopamine synthesis and is therefore expected to be expressed both in the tyrosine hydroxylase-positive JG cells as well as the raphe afferents.Uz et al. (2002) reported AANAT mRNA in the OB, but its location was not immediately apparent; our PCR results suggest that AANAT mRNA, like the melatonin receptor mRNAs, is expressed at low levels. The advantage of local melatonin synthesis isn't clear in the OB; melatonin may be valuable as a free-radical scavenger or as an additional paracrine neurotransmitter after serotonin is released into the OB.

Fluctuations in melatonin receptor mRNAs may not relate to changes in protein concentration, as previously reported for MT1R fluctuations in the SCN (Poirel et al., 2002). The size of the MT2R peaks (more than 8-fold and 12-fold, respectively) hours before darkness suggests that more melatonin receptors would be present closer to the onset of darkness, allowing some time for protein translation and insertion into the membrane. Fluctuations in TPH2 may be signal changes in the dorsal raphe nuclei, while AADC and HIOMT mRNA changes are likely responses to signals from the SCN or signals from the OB's own pacemaking system. Fluctuations in TPH1 and TPH2 have been previously reported in the retina (Liang et al., 2004), though the effects of these fluctuations aren't yet clear.

The anti-melatonin receptor antibodies used in this study included some that had been previously published in the literature. The MT2R antibody from Novus identified some

protein that functioned as another histological marker for JG cells, bringing the number of JG cell histological markers to 12, but the protein that it bound wasn't identified, though the staining pattern was very similar to the one reported for melatonin-related receptor (GPR50) in the OB (Drew et al., 2001). We also noted that these antibodies, while previously published in several studies, did not appear to be specific for melatonin receptors, as labeling was identical between the OB, our positive control, and our negative controls. Previous studies utilizing these antibodies may need to be revisited due to the specious nature of these anti-melatonin receptor antibodies.

4 Conclusions

Melatonin receptors are present in the rat MOB and mediate transcriptional, translational, and electrical effects within MOB cells. The final enzyme in melatonin biosynthesis is present in the MOB and suggests that melatonin may be locally synthesized from exogenous serotonin.

Acknowledgments

The authors thank C. Badland for assistance in generating figures, R. Didier, C. Helena, C. Pye, B. Washburn, and K. Calvin for technical assistance. This work was supported by the US National Institute of Health (NIH) [T32 DC00044] and intramural funding from the Program in Neuroscience at Florida State University.

Abbreviations

K^+	potassium
I-mel	2-iodomelatonin
TPH1	tryptophan hydroxylase isoform 1
TPH2	tryptophan hydroxylase isoform 2
AADC	aromatic L-amino acid decarboxylase
AANAT	arylalkylamine-N-acetyltransferase
HIOMT	hydroxyindole-O-methyltransferase
ASMT	acetylserotonin methyltransferase
MT1R	melatonin receptor 1
MT2R	melatonin receptor 2
MT1R-KO	melatonin receptor 1 knock-out mouse
MT2R-KO	melatonin receptor 2 knock-out mouse
OB	olfactory bulb
JG	juxtaglomerular cell
PG	periglomerular cell
ET	external tufted cell
SA	short-axon cell
GL	glomerular layer
MCL	mitral cell layer
GCL	granule cell layer

EPL	external plexiform layer
ONL	olfactory nerve layer
GAPDH	glyceraldehyde-3-phosphate dehydrogenase
PCR	polymerase chain reaction
qPCR	quantitative PCR
SDS-PAGE	sodium dodecyl sulfate polyacrylamide gel electrophoresis
SCN	suprachiasmatic nucleus of the hypothalamus
Ni-DAB	nickel-diaminobenzidine
IHC	immunohistochemistry
(GABA)	gamma-amino butyric acid
FIHC	fluorescent IHC

References

Berkowicz DA, Trombley PQ. Dopaminergic modulation at the olfactory nerve synapse. Brain Res. 2000; 855:90–99. [PubMed: 10650134]

Blakemore LJ, Resasco M, Mercado MA, Trombley PQ. Evidence for Ca^{2+}-permeable AMPA receptors in the olfactory bulb. Am J Physiol Cell Physiol. 2006; 290:C925–C935. [PubMed: 16267106]

Briñón JG, Arévalo R, Crespo C, Bravo IG, Okazaki K, Hidaka H, Aijón J, Alonso JR. Neurocalcin immunoreactivity in the rat main olfactory bulb. Brain Res. 1998; 795:204–214. [PubMed: 9622632]

Corthell JT, Fadool DA, Trombley PQ. Connexin and AMPA receptor expression changes over time in the rat olfactory bulb. Neurosci. 2012; 222:38–48.

Drew JE, Barrett P, Mercer JG, Moar KM, Canet E, Delagrange P, Morgan PJ. Localization of the melatonin-related receptor in the rodent brain and peripheral tissues. J Neuroendocrinol. 2001; 13:453–458. [PubMed: 11328456]

Dubocovich ML, Delagrange P, Krause DN, Sugden D, Cardinali DP, Olcese J. International Union of Basic and Clinical Pharmacology. LXXV. Nomenclature, classification, and pharmacology of G protein-coupled melatonin receptors. Pharmacol Rev. 2010; 62:343–380. [PubMed: 20605968]

Gómez-Corvera A, Cerrillo I, Molinero P, Naranjo MC, Lardone PJ, Sanchez-Hidalgo M, Carrascosa-Salmoral MP, Medrano-Campillo P, Guerrero JM, Rubio A. Evidence of immune system melatonin production by two pineal melatonin deficient mice, C57BL/6 and Swiss strains. J Pineal Res. 2009; 47:15–22. [PubMed: 19522737]

Granados-Fuentes D, Ben-Josef G, Perry G, Wilson DA, Sullivan-Wilson A, Herzog ED. Daily rhythms in olfactory discrimination depend on clock genes but not the suprachiasmatic nucleus. J Biol Rhythms. 2011; 26:552–560. [PubMed: 22215613]

Granados-Fuentes D, Prolo LM, Abraham U, Herzog ED. The suprachiasmatic nucleus entrains, but does not sustain, circadian rhythmicity in the olfactory bulb. J Neurosci. 2004; 24(3):615–619. [PubMed: 14736846]

Guillemin I, Becker M, Ociepka K, Friauf E, Nothwang HG. A subcellular prefractionation protocol for minute amounts of mammalian cell cultures and tissue. Proteomics. 2005; 5:35–45. [PubMed: 15602774]

Hoffman GE, Le WW, Sita LV. The importance of titrating antibodies for immunocytochemical methods. Chapter 2: Unit 2.12. Curr Protoc Neurosci. 2008

Hunt AE, Al-Ghoul WM, Gillette MU, Dubocovich ML. Activation of MT2 melatonin receptors in rat suprachiasmatic nucleus phase advances the circadian clock. Am J Physiol Cell Physiol. 2001; 280:C110–C118. [PubMed: 11121382]

Hwang IK, Kang TC, Lee JC, Lee IS, Park SK, An SJ, Jeong YG, Seo JG, Oh YS, Won MH. Agerelated change of calbindin D-28k immunoreactive neurons in the rat main olfactory bulb. Neurosci Lett. 2002; 326(3):159–162. [PubMed: 12095646]

Inyushkin AN, Bhumbra GS, Gonzalez JA, Dyball REJ. Melatonin modulates spike coding in the rat suprachiasmatic nucleus. J Neuroendocrinol. 2007; 19:671–681. [PubMed: 17680882]

Ishii H, Nobuyuki T, Kobayashi M, Kato M, Sakuma Y. Gene structures, biochemical characterization and distribution of rat melatonin receptors. J Physiol Sci. 2009; 59:37–47. [PubMed: 19340560]

Itoh MT, Takahashi N, Abe M, Shimizu K. Expression and cellular localization of melatoninsynthesizing enzymes in the rat lens. J Pineal Res. 2007; 42:92–96. [PubMed: 17198543]

Jin X, von Gall C, Pieschl RL, Gribkoff VK, Stehle JH, Reppert SM, Weaver DR. Targeted disruption of the mouse Mel1b melatonin receptor. Molec Cell Biol, Feb. 2003:1054–1060.

Kamphuis W, Cailotto C, Dijk F, Bergen A, Buijs RM. Circadian expression of clock genes and clock-controlled genes in the rat retina. Biochem Biophys Res Comm. 2005; 330:18–26. [PubMed: 15781226]

Kosaka T, Kosaka K. “Interneurons” in the olfactory bulb revisited. Neurosci Res. 2011; 69:93–99. [PubMed: 20955739]

Krause DN, Dubocovich ML. Melatonin receptors. Annu Rev Pharmacol Toxicol. 1991; 31:549–568. [PubMed: 1648339]

Lee B, Li A, Hansen KF, Cao R, Yoon JH, Obrietan K. CREB influences timing and entrainment of the SCN circadian clock. J Biol Rhythms. 2010; 25(6):410–420. [PubMed: 21135157]

Liang J, Wessel JH III, Iuvone PM, Tosini G, Fukuhara C. Diurnal rhythms of tryptophan hydroxylase 1 and 2 mRNA expression in the rat retina. Neurorep. 2004; 15(9):1497–1500.

Liu S, Aungst JL, Puche AC, Shipley MT. Serotonin modulates the population activity profile of olfactory bulb external tufted cells. J Neurophysiol. 2012; 107:473–483. [PubMed: 22013233]

Liu C, Weaver DR, Jin X, Shearman LP, Pieschl RL, Gribkoff VK, Reppert SM. Molecular dissection of two distinct actions of melatonin on the suprachiasmatic circadian clock. Neuron. 1997; 19:91–102. [PubMed: 9247266]

Ma J, Lowe G. Calcium permeable AMPA receptors and autoreceptors in external tufted cells of rat olfactory bulb. Neurosci. 2007; 144:1094–1108.

McLean JH, Shipley MT. Serotonergic afferents to the rat olfactory bulb: 1. Origins and laminar specificity of serotonergic inputs in the adult rat. J Neurosci. 1987; 7(10):3016–3028. [PubMed: 2822862]

Michel S, Itri J, Colwell CS. Excitatory mechanisms in the suprachiasmatic nucleus: the role of AMPA/KA glutamate receptors. J Neurophysiol. 2002; 88:817–828. [PubMed: 12163533]

Nosjean O, Ferro M, Coge F, Beauverger P, Henlin JM, Lefoulon F, Fauchere JL, Delagrange P, Canet E, Boutin JA. Identification of the melatonin-binding site MT3 as the quinone reductase 2. J Biol Chem. 2000; 275(40):31311–31317. [PubMed: 10913150]

Pandi-Perumal SR, Srinivasan V, Maestroni GJM, Cardinali DP, Poeggeler B, Hardeland R. Melatonin: Nature’s most versatile biological signal? FEBS J. 2006; 273:2813–2838. [PubMed: 16817850]

Paul KN, Fukuhara C, Karom M, Tosini G, Albers HE. AMPA/kainate receptor antagonist DNQX blocks the acute increase of*Per2*mRNA levels in most but not all areas of the SCN. Molec Brain Res. 2005; 139:129–136. [PubMed: 15963600]

Petzold GC, Hagiwara A, Murthy VN. Serotonergic modulation of odor input to the mammalian olfactory bulb. Nat Neurosci. 2009; 12(6):784–791. [PubMed: 19430472]

Pimentel DO, Margrie TW. Glutamatergic transmission and plasticity between olfactory bulb mitral cells. J Physiol. 2008; 586.8:2107–2119. [PubMed: 18276730]

Poirel V-J, Masson-Pévet M, Pevét P, Gauer F. MT1 melatonin receptor mRNA expression exhibits a circadian variation in the rat suprachiasmatic nuclei. Brain Res. 2002; 946:64–71. [PubMed: 12133595]

Resuehr D, Spiess A-N. A real-time polymerase chain reaction-based evaluation of cDNA synthesis priming methods. Anal Biochem. 2003; 322:287–291. [PubMed: 14596842]

Ribelayga C, Gauer F, Pévet P, Simonneaux V. Distribution of hydroxyindole-O-methyltransferase mRNA in the rat brain: an in situ hybridization study. Cell Tissue Res. 1998; 291:415–421. [PubMed: 9477298]

Sambrook, J.; Russell, D. Molecular Cloning. 3rd edition. Long Island: Cold Spring Harbor Press; 2001.

Schindler J, Jung S, Niedner-Schatteburg G, Friauf E, Nothwang HG. Enrichment of integral membrane proteins from small amounts of brain tissue. J Neural Transm. 2006; 113:995–1013. [PubMed: 16835696]

Schoppa NE, Westbrook GL. AMPA autoreceptors drive correlated spiking in olfactory bulb glomeruli. Nature Neurosci. 2002; 5(11):1194–1202. [PubMed: 12379859]

Sharkey JT, Puttaramu R, Word RA, Olcese J. Melatonin synergizes with oxytocin to enhance contractility of human myometrial smooth muscle cells. J Clin Endocrinol Metab. 2009; 94(2): 421–427. [PubMed: 19001515]

Sugden D. Comparison of circadian expression of tryptophan hydroxylase isoform mRNAs in the rat pineal gland using real-time PCR. J Neurochem. 2003; 86:1308–1311. [PubMed: 12911638]

Trombley, PQ.; Blakemore, LJ. Mammalian Olfactory Bulb Neurons. In: Haynes, LW., editor. The Neuron in Tissue Culture. Sussex: John Wiley & Sons, Ltd; 1999. p. 585-592.

Uz T, Qu T, Sugaya K, Manev H. Neuronal expression of arylalkylamine N-acetyltransferase (AANAT) mRNA in the rat brain. Neurosci Res. 2002; 42:309–316. [PubMed: 11985883]

Yang X-F, Miao Y, Ping Y, Wu H-J, Yang X-L, Wang Z. Melatonin inhibits tetraethylammonium-sensitive potassium channels of rod on type bipolar cells via MT2 receptors in rat retina. Neurosci. 2011; 173:19–29.

Yeung YG, Stanley ER. A solution for stripping antibodies from polyvinylidene fluoride immunoblots for multiple reprobing. Anal Biochem. 2009; 389:89–91. [PubMed: 19303392]

Zawilska JB, Skene DJ, Arendt J. Physiology and pharmacology of melatonin in relation to biological rhythms. Pharmacol Rep. 2009; 61:383–410. [PubMed: 19605939]

Zeman M, Herichova I. Melatonin and clock genes expression in the cardiovascular system. Front Biosci (Schol Ed). 2013; 5:743–753. [PubMed: 23277083]

Zhao W-J, Zhang M, Miao Y, Yang X-L, Wang Z. Melatonin potentiates glycine currents through a PLC/PKC signalling pathway in rat retinal ganglion cells. J Physiol. 2010; 588.14:2605–2619. [PubMed: 20519319]

Highlights

- Melatonin receptors and HIOMT are present in the olfactory bulb
- OB cells have transcriptional responses to melatonin application
- A subset of OB cells has electrical responses to melatonin application

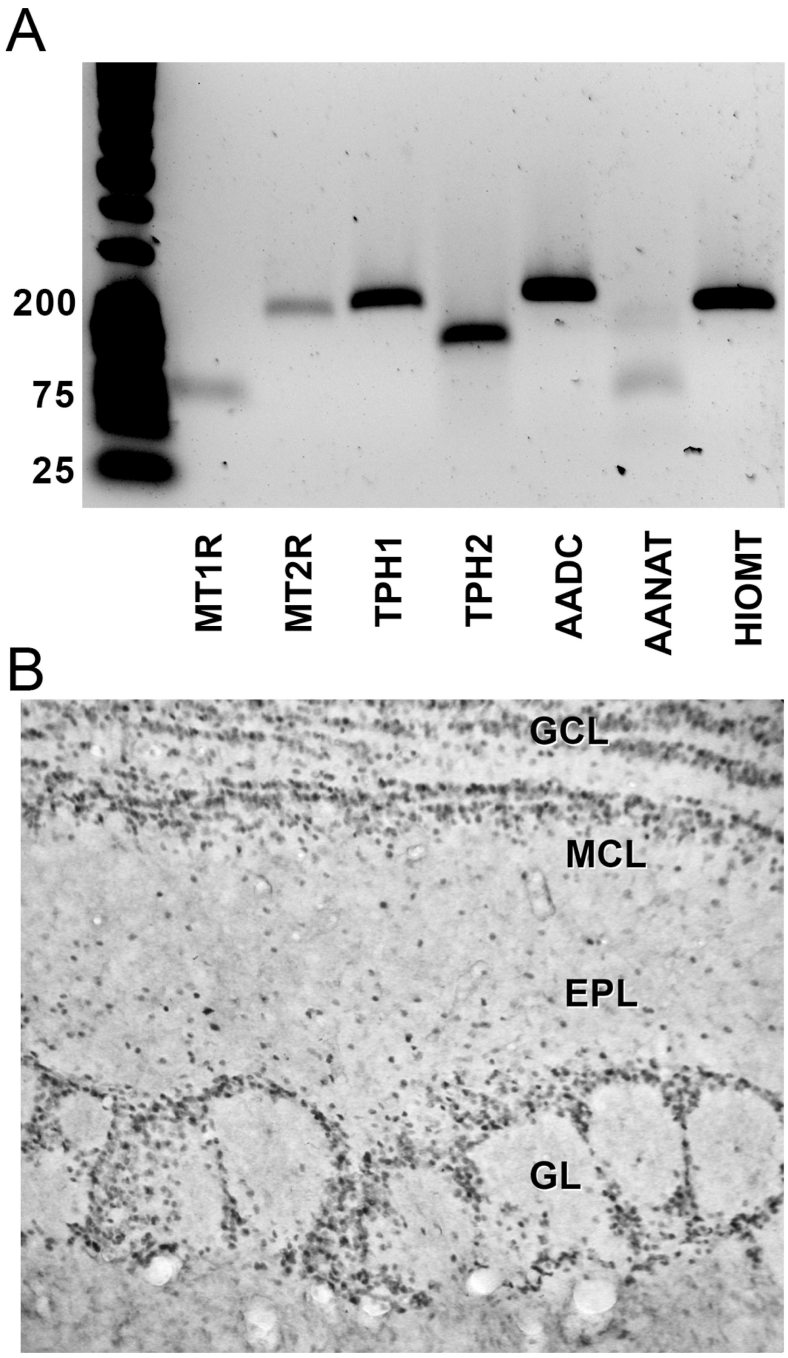

Figure 1.

Messenger RNAs encoding melatonin receptors and melatonin synthesis enzymes are present in the olfactory bulb (OB). A: PCR and gel electrophoresis of melatonin receptors and synthesis enzymes. From left to right: 25/100 bp marker, melatonin receptor 1, melatonin receptor 2, tryptophan hydroxylase 1, tryptophan hydroxylase 2, aromatic L-amino acid decarboxylase, arylalkylamine N-acetyltransferase, and hydroxyindole-O-methyltransferase. Messenger RNA encoding both melatonin receptors and all the melatonin synthesis enzymes are present in OB extracts, though MT1R, MT2R, and AANAT appear to be expressed at low levels in OB samples. Numbers on the left are bp weights. N = 5. B: MT2R antibody immunoreactivity in the rat OB. Extensive staining can be seen in the

glomerular and granule cell layers of the OB; there is some staining in the plexiform layers and no staining in the mitral cell layer. N = 6, similar staining was observed for 5 wild-type mice and 3 MT2R-KO mice. GL = glomerular layer, EPL = external plexiform layer, MCL = mitral cell layer, GCL = granule cell layer.

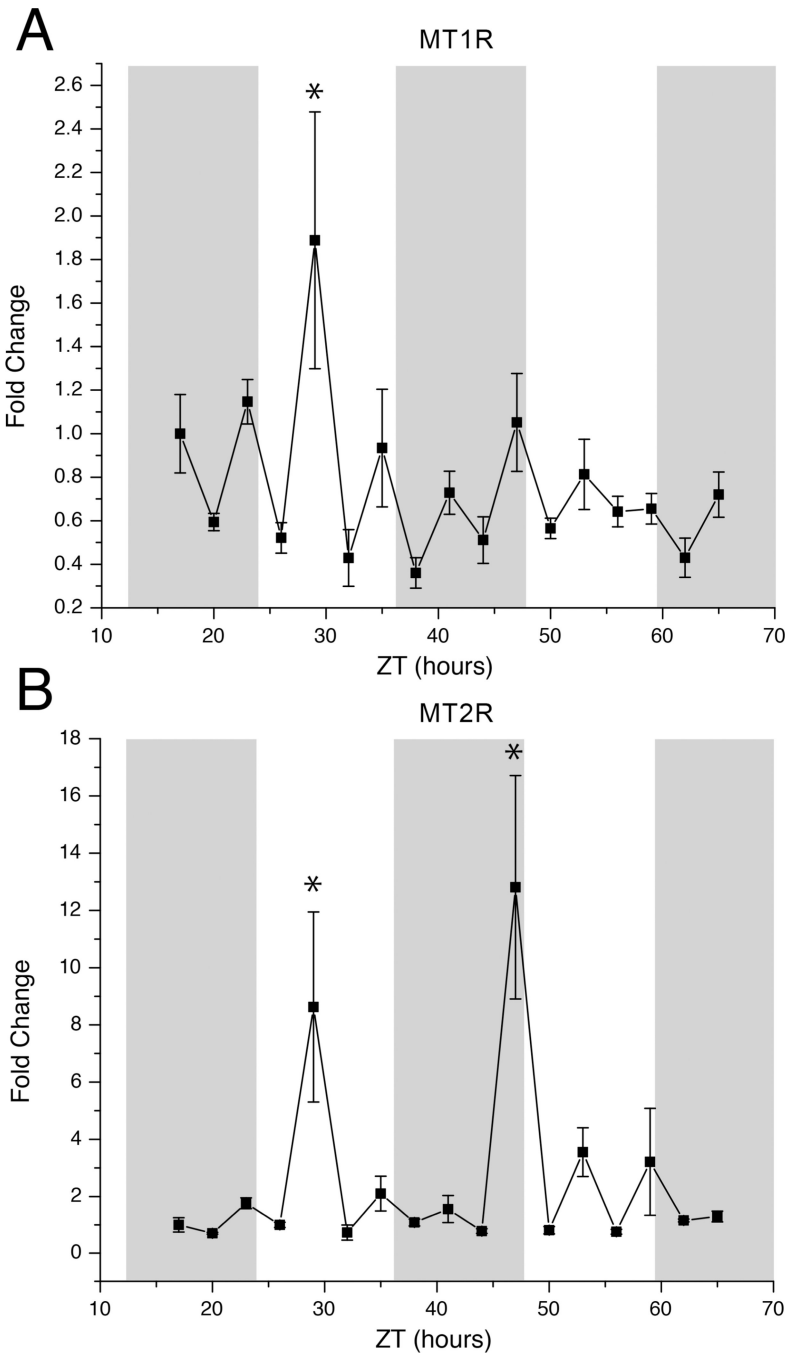

Figure 2.

Melatonin receptor mRNAs fluctuate across the light/dark cycle. A: Melatonin receptor 1 mRNA fluctuated in the first 24 hours, but those fluctuations did not return in the second 24-hour period tested. B: Melatonin receptor 2 mRNA fluctuated in both 24-hour periods tested, but those high fluctuations (8- to 13-fold changes, on average) did not occur at the same time points on the two respective days. Each point is the average +/− SEM. N = 4–6 individual animals per time point. Changes were statistically significant ($p < 0.05$) as assessed by Kruskal-Wallis and Dunn's tests. Shaded bars reflect the dark phase. Asterisks identify groups that were statistically significantly different from other groups, as assessed by Dunn's post-hoc test.

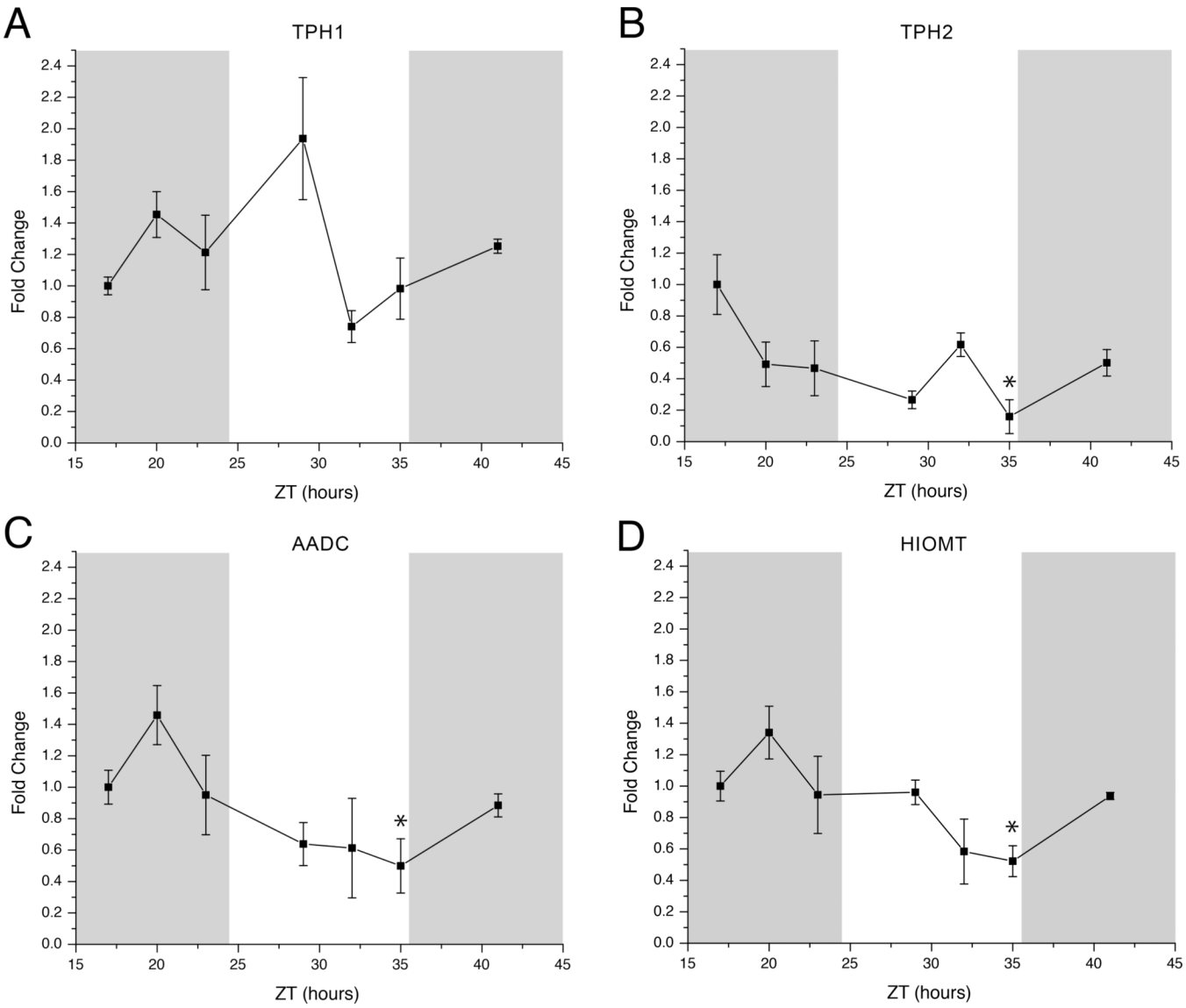

Figure 3.

Tryptophan hydroxylase (TPH), aromatic L-amino acid decarboxylase (AADC), and hydroxyindole-O-methyltransferase (HIOMT) mRNAs fluctuate across the light/dark cycle. A: Tryptophan hydroxylase, isoform 1 (TPH1) mRNA changed between light and dark phases and returned to baseline levels, but the results were not statistically significant. B: Tryptophan hydroxylase, isoform 2 (TPH2) mRNA fluctuated across the cycles but did not return to baseline. C: Aromatic L-amino acid decarboxylase (AADC) mRNA fluctuates across the light/dark cycle, returned to baseline, and was statistically significant. D: Hydroxyindole-O-methyltransferase (HIOMT) mRNA fluctuated across the light/dark cycle and returned to baseline levels; those fluctuations were statistically significant and correlated to AADC mRNA fluctuations depicted in C. Each point is the average +/− SEM. N = 4–6 individual animals per time point. Statistical significance ($p < 0.05$) was assessed by Kruskal-Wallis and Dunn's tests. Shaded bars reflect the dark phase. Asterisks identify groups that were statistically significantly different from other groups, as assessed by Dunn's post-hoc test.

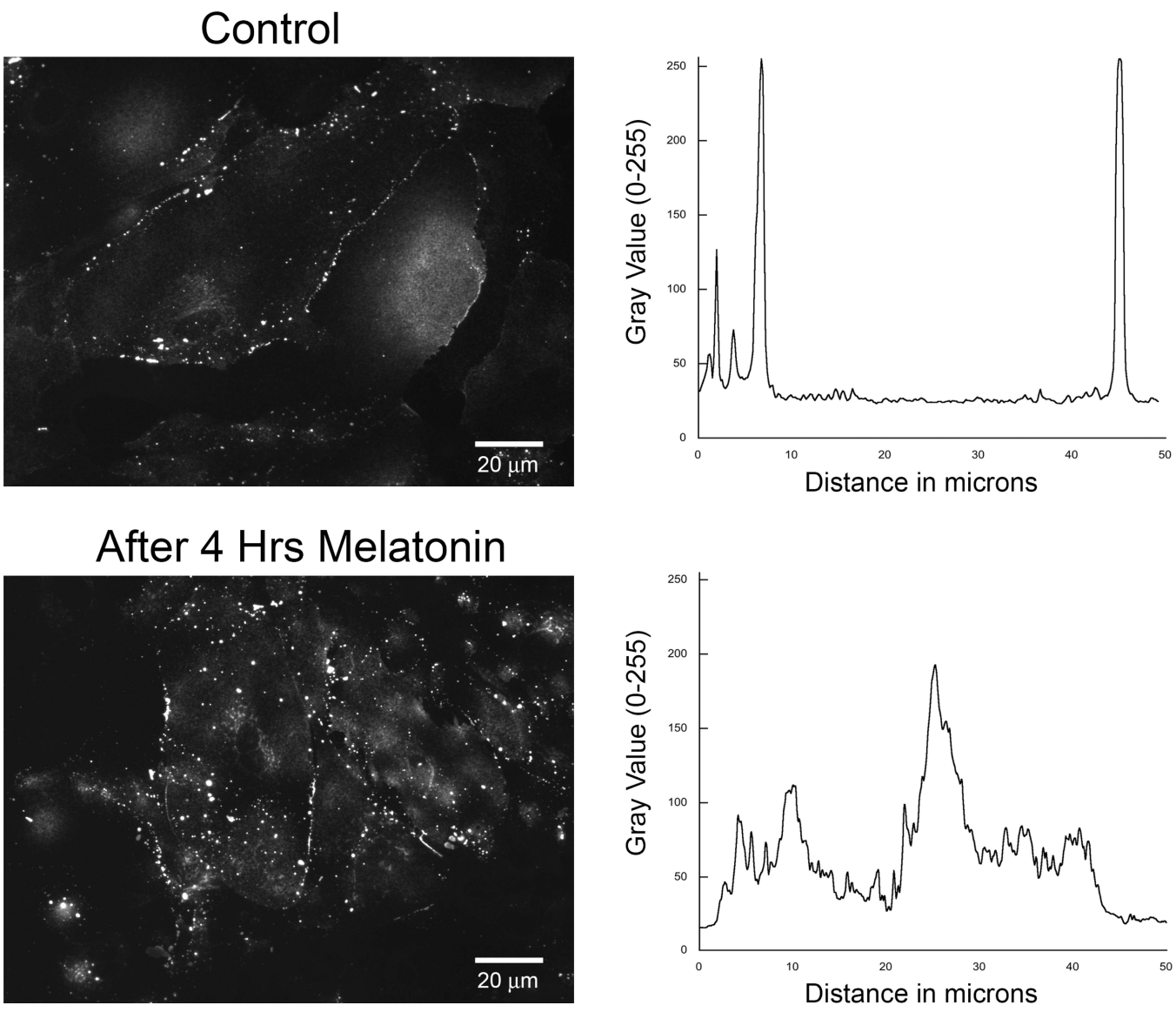

Figure 4.

Olfactory bulb astrocyte cultures respond to iodomelatonin. Top: control cultures treated with fresh medium. Bottom: cultures treated with 3 nM iodomelatonin in fresh medium. Connexin43 immunoreactivity increased in the treated cultures compared to controls. The control astrocytes appear to express connexins primarily in discrete locations, while expression was more diffuse after melatonin treatment. To the right of each picture is the analysis from the ImageJ program, indicating that, when a line was drawn across the image, there was more diffuse immunoreactivity in the treated cultures compared to controls. Gray value refers to the intensity of the pixels across that line, where a higher gray value indicates increased fluorescence than a lower gray value. N = 3.

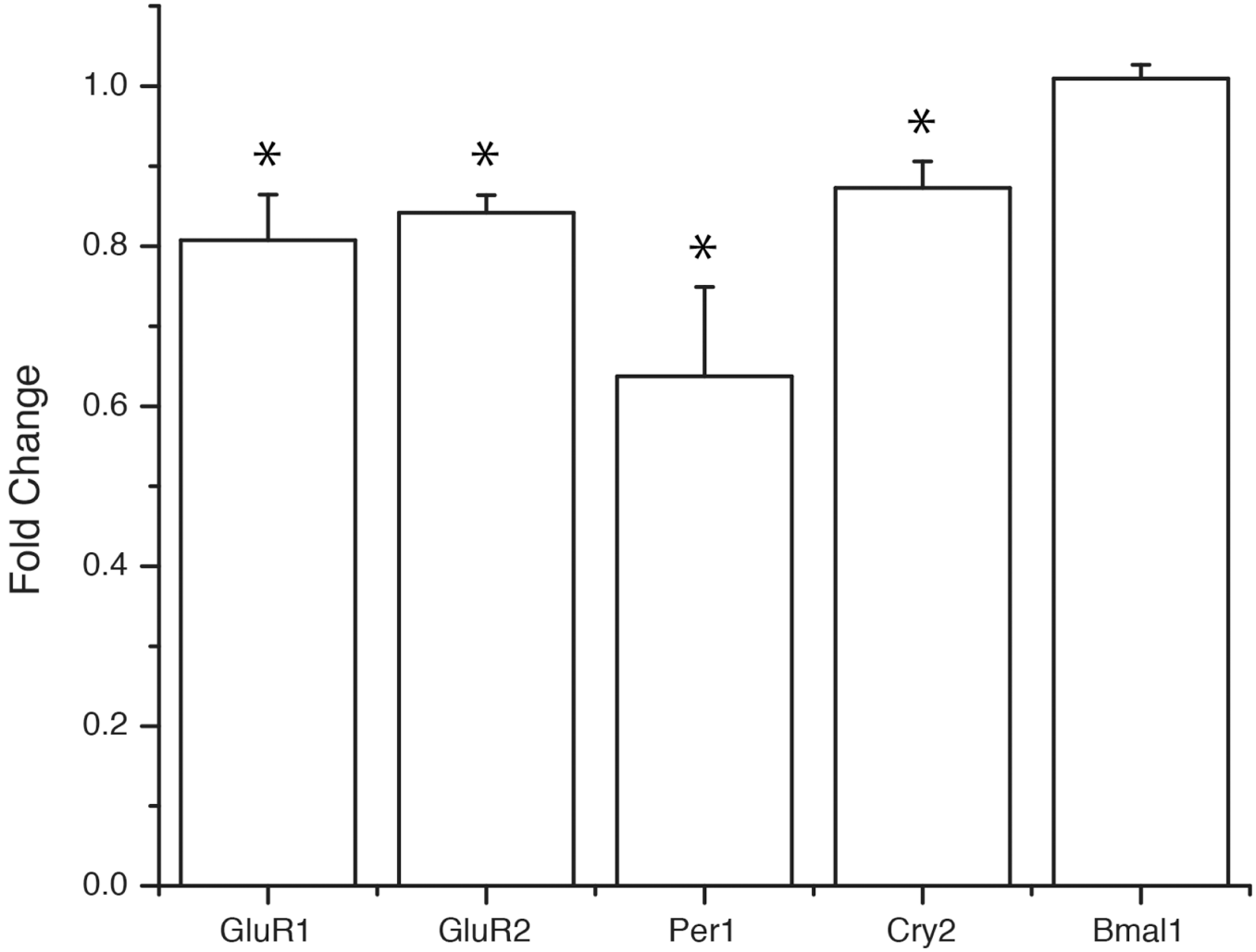

Figure 5.
Olfactory bulb slices respond to iodomelatonin. The histogram shows the fold change of the mRNA, compared to untreated controls (set at 1.0). *GluR1, GluR2, Per1*, and *Cry2* mRNAs decreased compared to their controls, while *Bmal1* mRNA did not appear to change in response to the experimental treatment. Statistical significance ($p < 0.05$) noted by asterisks above bars. Bars are + SEM. N = 4.

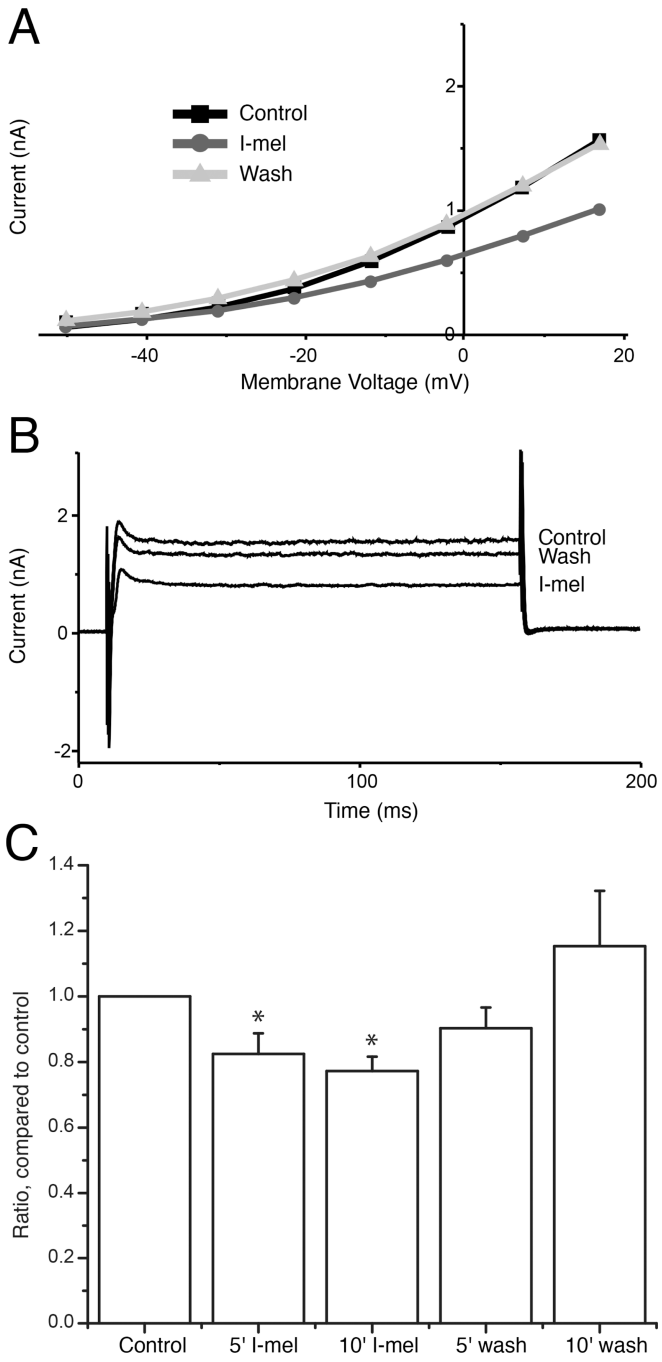

Figure 6.

A subset of juxtaglomerular cells respond to iodomelatonin. A: I-V curve of voltage step data. 5 minutes of iodomelatonin (I-mel) application results in a decreased current that recovers after 5 minutes of washout. B: Representative traces from the voltage step protocol. I-mel application decreases K^+ currents to 82 +/− 6% of control within 5 minutes of exposure, to 77 +/− 4% of control after 10 minutes of exposure. K^+ current recovers to 90 +/− 6% of control after 5 minutes of washout. C: Histogram showing current changes compared to control. Asterisks above bars denote statistical significance (t-test, $p < 0.05$). Bars are + SEM. N = 3 for washout, n = 9 had no effect.

Table 1

Primer sets used in this study.

Gene	Forward	Reverse	Product size (bp)
Melatonin receptor 1 (MT1R)	GGG GTC TTA CTG CTT TCT CTT	CCG CTC CAA CAC TAT GCT G	83
Melatonin receptor 2 (MT2R)	CCT TTT GCT ACC TGC GAA	TTG CCT CTG GAT TGA TGG	192
Aromatic L-amino acid decarboxylase (AADC)	GAA GAG GGA AGG AGA TGG TGG ATT	GCG AAG AAG TAG GGG CTG TGC	211
Tryptophan hydroxylase isoform 1 (TPH1)	CAA GGA GAA CAA AGA CCA TTC	ATT CAG CTG TTC TCG GTT GAT	208
Tryptophan hydroxylase isoform 2 (TPH2)	CGC CGA CCA CCC AGG ATT	CCC GAA ACA CAA CAC CCC AAG T	149
Arylalkylamine N-acetyltransferase (AANAT)	GCG AGG GTG GGA GTG ACA AG	TGG GGA CAG ACA GCA GCC	182
Hydroxyindole-O-methyltransferase (HIOMT)	TACGGGGACAGGAAGTTTTG	GTGCCACTTCTGGGTTCATT	198